Science of the Total Environment 864 (2023) 161009

Contents lists available at ScienceDirect

Science of the Total Environment

journal homepage: www.elsevier.com/locate/scitotenv

Zinc speciation and desorption kinetics in a mining waste impacted tropical soil amended with phosphate

Frederico Prestes Gomes [a,*], Matheus Bortolanza Soares [a], Hudson Wallace Pereira de Carvalho [b], Aakriti Sharma [c], Dean Hesterberg [c,d], Luís Reynaldo Ferracciú Alleoni [a]

[a] University of São Paulo, Luiz de Queiroz College of Agriculture, Av. Pádua Dias, 11, Piracicaba, São Paulo 13418-900, Brazil
[b] University of São Paulo, Center of Nuclear Energy in Agriculture, Av. Centenário, 303, Piracicaba, São Paulo 13416-000, Brazil
[c] Department of Soil Science, North Carolina State University, Raleigh, NC 27695, USA
[d] Brazilian Synchrotron Light Laboratory (LNLS), Brazilian Center for Research in Energy and Materials (CNPEM), R. Giuseppe Máximo Scolfaro, Campinas 13083-100, Brazil

HIGHLIGHTS

- In situ remediation was evaluated for Zn immobilization in mining soil.
- μ-XRF and μ-XANES were combined to investigate Zn in phosphate-amended soil.
- Phosphate increased Zn desorption and reduced Zn content in the residual fraction.
- Phosphate reduced recalcitrant Zn species such as gahnite and montmorillonite.

GRAPHICAL ABSTRACT

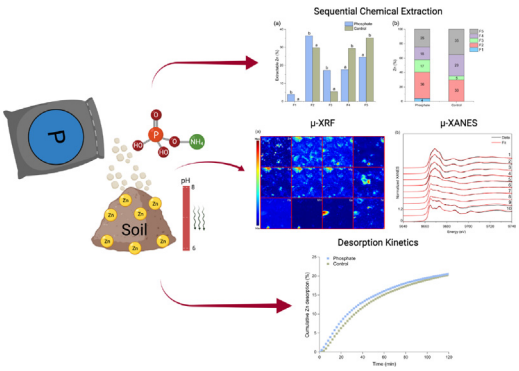

ARTICLE INFO

Editor: Baoliang Chen

Keywords:
X-ray absorption near-edge structure
Soil pollution
Remediation
Mining

ABSTRACT

Mining is an important component of the Brazilian economy. However, it may also contribute to environmental problems such as the pollution of soils with zinc and other potentially toxic metals. Our objective was to evaluate changes in the chemical speciation and mobility of Zn in a soil amended with phosphate. Soil samples were collected from a deactivated mining area in the state of Minas Gerais, Brazil, and amended with $NH_4H_2PO_4$ saturated with deionized water to 70 % of maximum water retention and incubated at 25 ± 2 °C in open containers for 60 days. The soil was chemically and mineralogically characterized, and sequential extraction, desorption kinetics, and speciation were carried out using synchrotron bulk-sample and micro–X-ray Absorption Near-Edge Structure (XANES/μ-XANES) spectroscopy at the Zn K-edge, and X-ray fluorescence microprobe analysis (μ-XRF). The combination of μ-XRF and μ-XANES techniques made it possible to identify Zn hotspots in the main species formed after phosphate remediation. The best fit combination for bulk XANES and μ-XANES was observed in Zn-montmorillonite, Zn-kerolite, Zn-ferrihydrite, and gahnite. In the course of phosphate treatment, gahnite, Zn layered double hydroxides (Zn-LDH), $Zn_3(PO_4)$, and ZnO were identified by bulk XANES, while Zn-ferrihydrite, Zn-montmorillonite, and scholzite were identified by μ-XANES. Zinc in the phosphate-amended soil had the strongest partial correlations ($r' > 0.05$) with Ni, Co, Fe, Cr, Mn, Si, P, Cd, Pb, and Cd, while the unamended soil showed the strongest correlation with Cu, Pb, Fe, and Si. The application of $NH_4H_2PO_4$ altered Zn speciation and favored an increase in Zn desorption. The most available Zn contents after phosphate amendment were correlated with the release of exchangeable Zn fractions, associated with carbonate and organic matter.

* Corresponding author.
E-mail address: fred.prestes@gmail.com (F.P. Gomes).

http://dx.doi.org/10.1016/j.scitotenv.2022.161009
Received 23 May 2022; Received in revised form 29 November 2022; Accepted 13 December 2022
Available online 19 December 2022

1. Introduction

The >2647 mining areas in Brazil account for almost 5 % of Brazil's Gross Domestic Product and 20 % of total employment (Brasil, 2011). Mining and smelting activities, however, are projected to generate 11.4 million metric tons of waste between 2010 and 2030 (Brasil, 2011). In 2014, Brazil produced 170 kt of Zn, which is approximately 1.5 % of world production (Filho et al., 2015). Part of this production is from mining areas in the Vazante region, located in the state of Minas Gerais (Soares Monteiro et al., 2006), home to one of the world's major known deposits of non-sulfide zinc (Hitzman et al., 2003).

Mining waste typically has a high content of potentially toxic elements such as zinc (Zn), lead (Pb), and cadmium (Cd) that are usually found on the surface of soils after mining (Steinnes, 1995). Once mobilized in soils, these elements can be transferred to groundwater and plants, and present a potential threat to human health (Sharma et al., 2018). Although Zn is essential to the metabolism of plants and animals (Roberts et al., 2002), in excess it can lead to toxicity.

The majority of soils found in the humid tropics are particularly unique because they are highly weathered (e.g., Oxisols) and rich in (hydr)oxide minerals which, for the main part, have a pH-dependent surface charge (McBride, 1994). These (hydr)oxide minerals immobilize heavy-metal cations such as Zn^{2+}, Pb^{2+}, Cu^{2+}, Cd^{2+} (Appel, 2002), and oxyanions such as $H_2AsO_4^-$ and $HSeO_3^-$ over a wide pH range (Goh and Lim, 2004). The soils found in mines are usually at circumneutral pH (Fellet et al., 2011). However, pH can decrease over time due to high precipitation and temperature, and thereby increase the availability of toxic trace elements (McBride, 1994).

Because excavation and deposition in landfills are economically unfeasible in emerging countries like Brazil, innovative and cost-effective strategies are needed to reduce the risks associated with heavy metals. In-situ remediation is an established, cost-effective approach for immobilizing contaminants in their place of origin. Amendments found to be effective for immobilizing metal contaminants in non-tropical soils include phosphate (Baker et al., 2014; Seshadri et al., 2017), alkaline materials (Basta and McGowen, 2004; Sik Ok et al., 2011), biochar (Abdelhafez et al., 2014; Puga et al., 2015), and organic compounds (Nawab et al., 2016; Sidhu et al., 2016). These amendments are reported to reduce the environmental risks associated with heavy metals in soils by the formation of low soluble salts or precipitates and increased sorption (Lee et al., 2009).

Understanding the chemical speciation of heavy metals in soils is an important step towards rational use of such amendments to optimize their effectiveness. Synchrotron radiation techniques such as X-ray fluorescence microanalysis (μ-XRF) and X-ray Absorption Near-Edge Structure (XANES) are established suitable techniques for ascertaining metal speciation and their possible associations in complex environmental media due to their selectivity as regards elements studied and their high resolution. These techniques are state-of-art tools that can probe the local atomic structure of Zn in soils, minerals, and sediments (Manceau et al., 2000; Roberts et al., 2002; Scheinost et al., 2002; Voegelin et al., 2002).

Our hypothesis was that even with a reduction in pH, the application of ammonium phosphate would precipitate Zn in stable phases and thereby reduce the availability of Zn. Thus, we aimed to evaluate the chemical species of Zn formed after the application of $NH_4H_2PO_4$ and Zn desorption potential. We used synchrotron μ-XRF and μ-XANES, stirred-flow kinetic approach, and sequential extraction. The information provided in this study will be important to the formulation of new strategies for the in-situ stabilization of Zn in tropical soils impacted by mining waste.

2. Material and methods

2.1. Soil collection and characterization

Soil samples of a Technosol (anthropogenic soil) were collected from the surface layer (0–20 cm) in a Zn mining area located in Vazante, in the state of Minas Gerais, Brazil (close to geographical coordinates 17°59″ S, 46°54′ W). The uncontaminated soil below the Technosol is a Ferralsols by the FAO Classification System (WRB, 2014), and an Oxisol by the Soil Taxonomy (Soil Survey Staff, 2014). The soil was air-dried at room temperature and passed through a 2-mm sieve. Soil total organic C content was determined with a Shimadzu TOC-5000. The pseudo-total concentrations of Cd, Pb, and Zn in the soil sample were extracted according to the EPA3051a method (1:3 HCl/HNO_3, *v*/v) (USEPA, 2007) and quantified by inductively coupled plasma optical emission spectroscopy (ICP-OES; iCAP 6300, Thermo Scientific, USA).

Other chemical analyses (exchangeable ions and pH) followed the methods of Ingram and Anderson (1993). X-ray diffraction (XRD) was performed on the bulk soil, the clay, sand, and silt fractions. We also performed XRD in the clay fraction after both concentrating the iron oxides with 5 M NaOH (Kampf and Schwertmann, 1982), and applying treatment with sodium dithionite-citrate-bicarbonate (DCB) for removing the free iron oxides (Mehra and Jackson, 1960). More information about the XRD procedure can be found in the Supporting Information (SI) section.

2.2. Amendment and incubation

The soil was amended individually in triplicate with monobasic ammonium phosphate ($NH_4H_2PO_4$) (Sigma-Aldrich; high purity and solubility in water of 2.5 M). Phosphorus (P) was applied to the soil at 2:1 molar ratios of P relative to the sum of Pb, Cd, and Zn. This rate was based on the possible formation of precipitate $M_5(PO_4)_3OH$ (M = sum of Zn, Pb, and Cd) (Fang et al., 2012).

Teflon flasks with a volume of 0.5 L were used to perform the experiment. In each flask, 200 g of previously dried soil with a granulometry of <2 mm were added. The $NH_4H_2PO_4$ was dissolved in ultrapure water, and later the solution was applied on the soil surface to ensure the homogeneity of the application of $NH_4H_2PO_4$ in the soil and between treatments. After the $NH_4H_2PO_4$ application, the soil was incubated at 25 ± 2 °C for 60 days, and the soil moisture was maintained with additions of deionized water at 70 % of the maximum water-holding capacity every three days based on the loss of water mass.

2.3. Bulk XANES

Zinc-K edge XANES analysis was carried out at the XAFS2 beamline at the LNLS (Brazilian Synchrotron Light Laboratory), located in Campinas, state of São Paulo, Brazil. The measurements were taken in transmission mode using a Si (111) double crystal monochromator. Energy was calibrated using a Zn metal foil positioned between the second and the third ionization chambers. The soil samples were ground, and 150 mg was pressed into 5 mm diameter pellets in a 1.3 cm^2 area ~1.5 mm thick.

Three XANES spectra were collected per sample across the energy range of −130 to 340 eV relative to the Zn-K edge energy at 9659 eV. These spectra were energy calibrated, aligned, merged, and normalized by means of the Athena program in the IFEFFIT package. Linear combination fitting (LCF) analyses were plotted across an energy range of −20 to 80 eV relative to E_0 by a standard elimination procedure following Manceau et al. (2012) which was applied to find the best fit combination of standards to fit the sample spectra (Fig. 1). Additional information about the bulk XANES procedure and standards (Table A.1) utilized for the LCF analysis is in the SI Section.

2.4. Micro-XRF and Micro-XANES

Micro-XRF imaging and spectroscopy were applied to the phosphate-amended and unamended soil sample that was air-dried, ground, embedded in epoxy and prepared as thin sections each ~20 μm thick. For the P-amended soil, we used the Beamline (5-ID) sub-micron resolution X-ray spectroscopy (SRX) from the National Synchrotron Light Source II (NSLS-II), Brookhaven National Laboratory in Upton, New York, USA. This beamline had a focused spot of 1 μm × 0.7 μm controlled by Kirkpatrick−Baez mirrors and Si (111) horizontal double-crystal monochromator crystals.

Micro-XRF analysis was carried out using an incident beam energy of 15 keV and fluorescence signals were recorded by a three-element Si drift

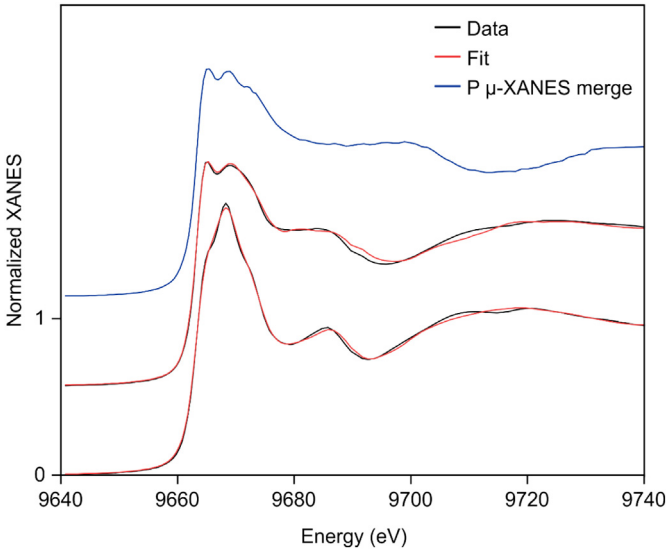

Fig. 1. Zinc K-edge (μ-)XANES spectra and overlaid linear combination fits from Table 2 for mining area soil samples amended with the treatments of phosphate.

detector. A 120 μm × 120 μm image of the sample was collected in step-scan mode using a step size of 1 μm and a 0.3 s dwell time. The μ-XRF mapping technique was used to image spatial distributions of Zn, Si, P, Ca, Fe, Al, Mg, K, Pb, Mn, Cu, and Ni.

For the unamended soil, the analyses were completed using μ-XRF and μ-XANES at the D09B-XRF Beamline at the LNLS. A focused 20 μm diameter spot size controlled by a KB mirror system and Si (111) crystal monochromator were used. Micro-XRF analysis was carried out using incident beam energy of 15 keV and the fluorescence signals were measured by a silicon drift detector (SDD; AXAS-A, KETEK GmbH, Germany). The image was collected across a 4000 × 3000 μm area of the sample, using a step size of 30 μm and 0.3 s dwell time. The μ-XRF mapping technique was used to image the distributions of Zn, Fe, and Si (Fig. A.1).

Zinc K-edge μ-XANES spectra were collected at ten points on the μ-XRF map in P-amended soil and three points on the μ-XRF map in unamended soil. Five μ-XANES spectra were collected per sample and were acquired across the energy range of −100 to 200 eV relative to the Zn K-edge energy at 9659 eV. The LCF analysis was carried out across an energy range of −20 to 80 eV and −20 to 40 eV relative to E_0 for both the P-amended and unamended soil, respectively. The fit results were obtained using the Manceau approach as described above for bulk XANES. Additional information about μ-XANES procedures and standards (Table A.1) utilized for the LCF analysis is in the SI section.

2.5. Statistical analyses of μ-XRF images

The μ-XRF intensity data normalized to the incoming X-ray intensity (I_0) were natural log-transformed to analyze a statistical relationship between Zn and other matrix elements (Ca, Cr, Co, Fe, Mn, Ni, Pb, Cd, P, Cu, Si). Simple Pearson correlation analyses were plotted together with partial correlation analyses to remove the effects of other confounding variables, i.e., co-localization of elements (Sharma et al., 2019). The total number of observations was 12,321 and correlations were considered significant at $\alpha = 0.05$. Correlation between element pairs may be weak but still significant because of the large number of observations. All statistical analyses were carried out using the R statistical software program (version 3.2.3).

2.6. Desorption experiments

Zinc desorption kinetics were carried out using a stirred-flow reactor equipped with a piston displacement pump designed for use in an HPLC system (LC-40B X3 HPLC/UHPLC, Shimadzu, Japan). A 12 mL stirred-flow chamber was used in these experiments to which 0.2 g of <2 mm sieved of each amended soil sample was added. Mehlich-3 solution (0.2 M CH_3COOH + 0.25 M NH_4NO_3 + 0.013 M HNO_3 + 0.015 M NH_4F + 0.001 M EDTA) was the desorption agent because it estimates the availability of heavy metals for plants (Hosseiwwnpur and Motaghian, 2015) and estimates bioaccessibility (Minca et al., 2014).

A 25-mm diameter cellulose filter membrane with a 0.45 μm pore size was used in the reaction chamber. The solution flowed through the chamber at a rate of 1 mL min^{-1} and the suspension in the reaction chamber was stirred at 300 rpm. The effluent was collected from the reactor at 2 min intervals over a period of 2 h, and Zn concentration was determined by ICP-OES (iCAP 6300, Thermo Scientific, USA). The desorption kinetics of Zn were calculated according to Yin et al. (1997) and plotted in cumulative Zn desorption percentages.

2.7. Sequential fractionation procedures

The sequential soil fractions were determined following the procedure developed by Silveira et al. (2006). The original method separates seven fractions although, in the present study, we used the following sequence of extractants which were designed to target various operational forms of metals: 0.1 M $CaCl_2$ for readily exchangeable Zn (F1); 1 M NaOAC (pH 5) for carbonates forms (F2); NaOCl (pH 8.5) for organic-matter bound (F3); 0.2 M oxalic acid + 0.2 M NH_4 oxalate (pH 3) for iron-oxides bound (F4); and the residual (F5) was obtained after digestion applying the EPA3051a method (USEPA, 2007). The Zn concentration in each extraction solution was quantified using ICP-OES (iCAP 6300, Thermo Scientific, USA). The means of the Zn content extracted from each fraction were compared by *t*-test ($p < 0.05$).

3. Results

3.1. Soil characteristics

Soils from the mining area were considered hazardous on account of the concentrations of Zn, Pb, and Cd exceeding the intervention values adopted by the state of São Paulo for industrial or residential areas, namely, 10,000 mg Zn kg^{-1}, 4400 mg Pb kg^{-1}, and 14.0 mg Cd kg^{-1} (CETESB – Environmental Agency of São Paulo State, 2016) (Table 1). The unamended soil sample had a pH of 8.3, but the addition of the P amendment reduced the pH by up to two units. The XRD indicated the presence of goethite (α-FeO(OH)), hematite (Fe_2O_3), kaolinite ($Al_2Si_2O_5(OH)_4$), gibbsite ($Al(OH)_3$), muscovite ($KAl_3Si_3O_{10}(OH)_2$), clinochlore ($(Mg,Fe^{2+})_5Al_2Si_3O_{10}(OH)_8$), montmorillonite ($(Na,Ca)_{0,3}(Al,Mg)_2Si_4O_{10}(OH)_2{\cdot}n(H_2O)$), and quartz ($SiO_2$) (Fig. 2).

Table 1
Selected chemical properties of amended with phosphate and control soil samples from the mining area.

Treatments	pH H_2O	C	P	Exchangeable						Total		
				K	Na	Ca	Mg	H + Al	Al	Cd	Pb	Zn
		g kg^{-1}	mg kg^{-1}	$mmol_c$ kg^{-1}						mg kg^{-1}		
Control	8.3	16	90	0.9	0.08	183	215	0	0	98	4300	13,000
Phosphate	6.3	16	8991	0.4	0.13	79	186	166	119	111	4100	13,100

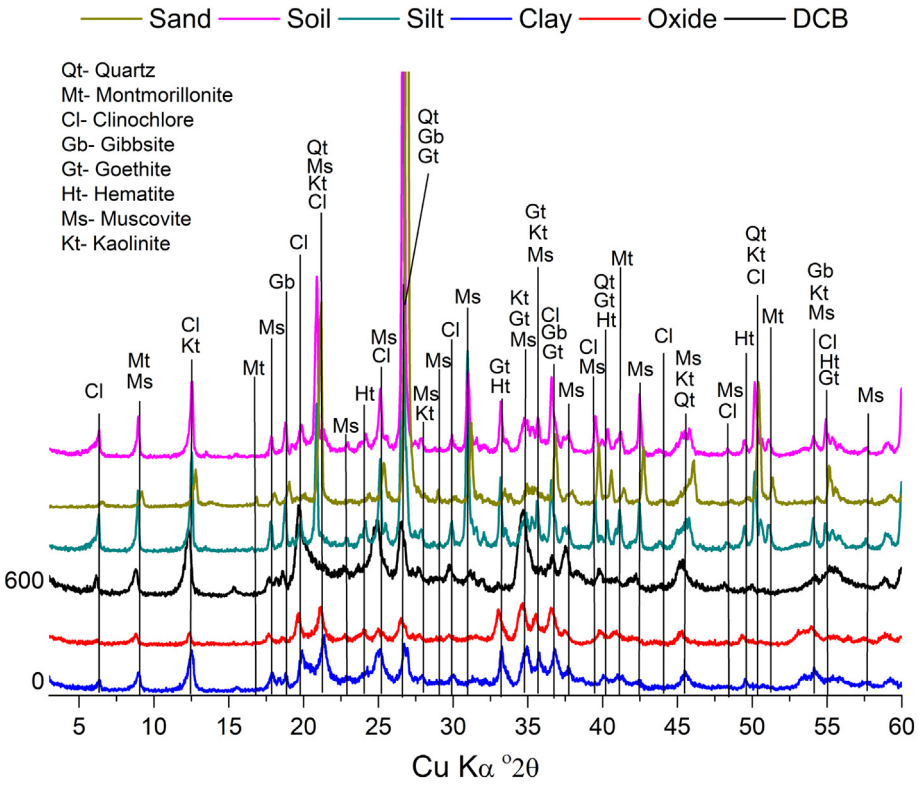

Fig. 2. XRD of the sand, silt, and clay fractions, and in the clay fraction after chemical treatments for removing iron oxides (DCB) and silicates (oxides).

3.2. Zinc speciation and elemental distribution

Zinc K-edge XANES spectra for the control (unamended) and amended soil samples from the mining area were nearly identical, except for the P-amended samples (Fig. 1). Consistent with the overlaid XANES spectra themselves, LCF results also showed similar best-fit combinations of standards to spectra for unamended soil samples (Table 2), including 26–30 % Zn-montmorillonite, 40–41 % Zn-kerolite ($Zn_{2.1}Mg_{0.9}Si_4O_{10}(OH)_2{\cdot}nH_2O$), 18–24 % Zn-ferrihydrite, and 10–14 % gahnite ($ZnAl_2O_4$). The best fit to the spectrum for the P-treated sample consisted of 20 % gahnite, 16 % Zn-LDH (Zn layered double hydroxides), 49 % $Zn_3(PO_4)_2$, and 15 % zincite (ZnO) (Table 2).

The μ-XRF images in the P-amended soil showed spatial distributions of Zn, Si, P, Ca, Fe, Al, Mg, K, Pb, Mn, Cu, and Ni (Fig. 3). The visible spatial pattern of Zn across the imaged area was not consistent with the pattern of any one single element, but it was consistent with fits to the ten μ-

Table 2
Combinations of standards yielding the best fits to zinc K-edge Micro and bulk-XANES spectra for mining area soil amended with phosphate for a linear-combination fitting (LCF) energy range of −20 to 80 eV relative to E_0 (first-derivative maximum).

Spots	$Zn_3(PO_4)_2$	ZnO	Gahnite	Zn-LDH	Zn-montmorillonite	Zn-ferrihydrite	Zn-kerolite	Scholzite	10^4 × R-factor[b]
	Proportion of standard ± uncertainty (%)[a]								
Micro-XANES - phosphate									
1				70 ± 4	30 ± 4				52.4
2	10 ± 1			69 ± 4	21 ± 4				46.2
3			15 ± 2	57 ± 6	28 ± 3				41.1
4				100					–
5	30 ± 2	21 ± 2	17 ± 2		8 ± 1	24 ± 3			14.2
6	29 ± 1	40 ± 2	12 ± 1					19 ± 3	6.7
7	24 ± 1	20 ± 1	22 ± 1					35 ± 2	7.9
8	19 ± 1	36 ± 2	14 ± 1					31 ± 1	5.1
9	35 ± 1		42 ± 1	23 ± 1					7.4
10	8 ± 2		72 ± 3			20 ± 4			6.8
Average	32 ± 2	12 ± 2	19 ± 3	27 ± 4	7 ± 2	4 ± 1		10 ± 2	18.3
Micro-XANES - control									
1			21 ± 2		41 ± 3	16 ± 2	20 ± 3		1.8
2			34 ± 2		48 ± 2	10 ± 2			7.2
3			41 ± 1		59 ± 1				9.4
Average			28 ± 3		49 ± 2	8 ± 1			5.6
Bulk-XANES									
Phosphate	49 ± 3	15 ± 1	20 ± 1	16 ± 1					11.7
Control			10 ± 1		26 ± 2	24 ± 2	40 ± 2		6.0

[a] All data have been re-normalized to sum to 100 %; uncertainties were calculated in Athena.
[b] R-factor is a measure of goodness of fit = $\Sigma(\text{data-fit})^2/\Sigma(\text{data})^2$.

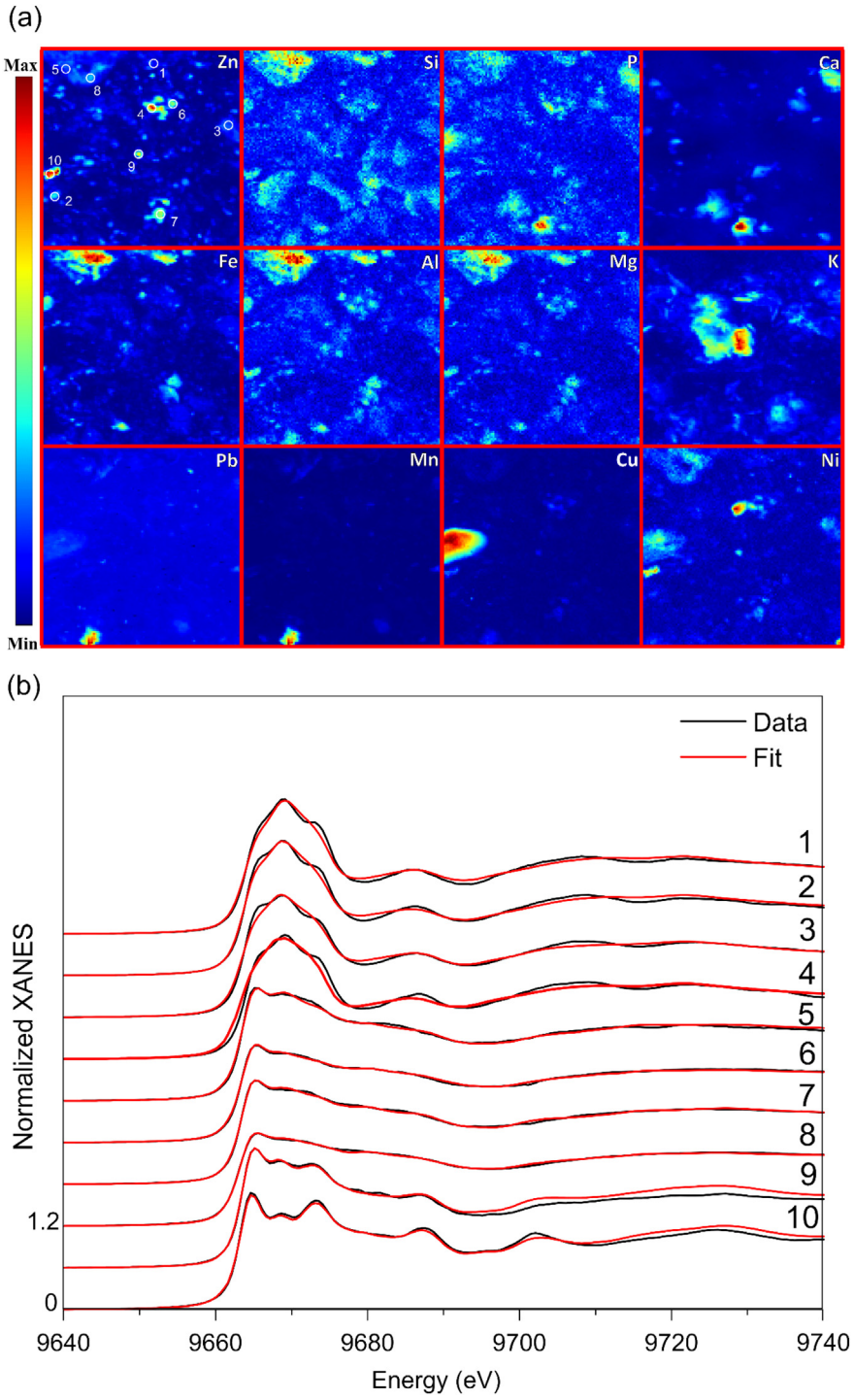

Fig. 3. (a) μ-XRF images showing spatial patterns of selected elements across a 120 μm × 120 μm area of a thin section of the phosphate-amended mine-soil sample; (b) Zn K-edge μ-XANES spectra taken at the 10 Zn spots labeled in (a) and overlaid fits from Table 2.

XANES spectra that included combinations of seven standards of varying composition across the ten spots analyzed (Fig. A.2). A Pb hotspot at the bottom of the image was not enriched in Zn but was co-localized with Mn. Zinc in hotspots 4 and 10 were co-localized with similar hotspots of Ni. In our study, Zn had strong significant correlation with Ni ($r = 0.62$), Co ($r = 0.56$), Fe ($r = 0.53$), and Cr ($r = 0.51$) (Table A.2). However, partial correlation that accounts for covariance between other elements showed the highest positive correlation with Ni ($r' = 0.56$) and Mn ($r' = 0.38$), and negative correlation with Pb ($r' = -0.29$).

The partial correlation coefficients decreased when compared to the Pearson correlation coefficient, implying that the simple Pearson correlation between Zn and Ni, Co, Fe, or Cr had a dependent spatial relationship with other co-localized elements which does not necessarily represent the spatial correlation between the elements. The partial correlations between element pairs (e.g., Zn-Co, Zn-Cr, and Zn-Cd) were weak but significant because of the large number of observations. The μ-XRF image for the unamended soil shows the spatial relationships between Zn, Cu, and Si (Fig. A.1). Zn had significant ($p < 0.02$) partial correlation coefficients significant only for Cu ($r' = 0.20$).

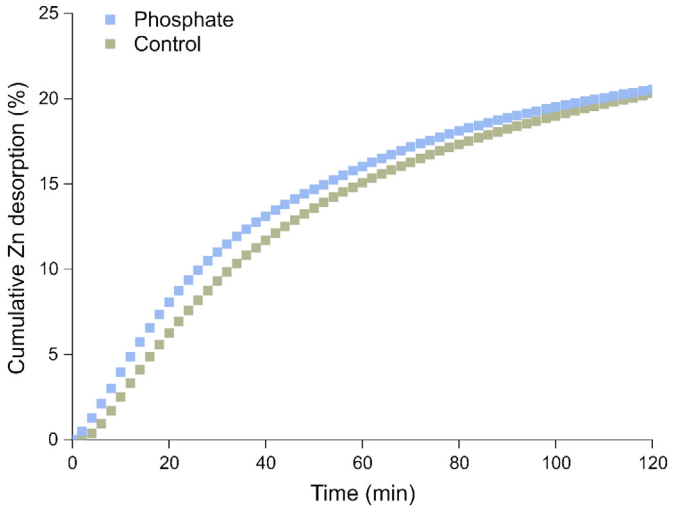

Fig. 4. Cumulative Zn desorption (% of the total Zn content on the soil) by Mehlich-3 extracting solution for amended and control samples from the mining area.

Micro-XANES spectra of the unamended soil collected from three spots confirmed the predominance of fit with Zn-montmorillonite (41–59 %) followed by gahnite (21–41 %) (Table 2). Spots 1 and 2 had a fit with Zn-ferrihydrite (10–16 %) and only spot 1 had a fit with Zn-kerolite (20 %). These data agreed with the LCF performed in the bulk XANES where the same species were identified (Table 2).

Micro-XANES spectra in the P-amended soil collected from ten spots varied (Fig. 3), and the best-fit combination of standards for all spots included 8–35 % $Zn_3(PO_4)_2$, 19–35 % scholzite ($CaZn_2(PO_4)_2{\cdot}2(H_2O)$), 21–40 % gahnite, 23–100 % Zn-LDH, 8–30 % Zn-montmorillonite, 20–24 % Zn-ferrihydrite (Table 2). The merging of these ten spectra was very similar to the spectra of the bulk XANES (Figs. 1 and A.1), whereas bulk XANES fit results did not show any fit with the standards of scholzite and Zn-montmorillonite. However, the Zn-montmorillonite standard had a significant fit in the μ-XANES (49 %) and bulk XANES (26 %) results of the unamended soil.

The greater proportion of gahnite in the fit was found in two "hotspots" (spots 9 and 10), consistent with results obtained by Kirpichtchikova et al. (2006). Considering the size of the microprobe beam (0.7 μm^2) and bulk beam (400 μm^2), ten μ-XANES spectra represented only 0.0001 % of the lateral sample area irradiated by the bulk beam. Nevertheless, the merged μ-XANES is qualitatively similar to the bulk XANES spectrum analyses and has the advantage of being able to identify species that cannot be deconvolved using bulk XANES.

3.3. Desorption kinetics and sequential extraction

The amount of Zn desorbed was normalized to the total soil Zn concentration and plotted as a function of time to compare the desorption behavior of treatments (Fig. 4). For each treatment, the amount of Zn desorbed after 2 h was 20.5 % for phosphate and 20.3 % for control. During the initial period of desorption (80 min) the P-amended soil had the highest desorption, coming close to equilibrium at around 2 h.

The P-amended soil was the only one with detectable amounts of Zn in F1 extracted with 0.1 M $CaCl_2$ and higher Zn contents in F2 (extracted with 1 M NaOAC pH 5) and F3 (extracted with 5 % NaOCl) - $p < 0.05$ (Fig. 5). The addition of P reduced the Zn extracted by 0.2 M oxalic acid + 0.2. M NH_4 oxalate (F4) and extracted according to EPA3051a (F5). As for the control, the application of P reduced the Zn content of F4 by 11 % in F4 and 10 % in F5.

4. Discussion

4.1. Effect of phosphate application on soil

The addition of phosphate reduced soil pH from 8.3 to 6.3 (Table 1), and this pH reduction may have partially increased the amount of Zn in the solution (Figs. 4 and 5). The Zn^{+2} ions are highly sensitive to changes in pH, ionic strength, free metal ion concentration, and the presence of competing ions (Sims, 1986). With the increase in acidity, Zn species such as ZnO may undergo dissolution, thereby increasing the concentration of "free" Zn in the solution (McBride and Blasiak, 1979).

The bulk Zn K-edge XANES spectrum for the unamended soil indicated Zn-kerolite (40 % of total Zn) and Zn-montmorillonite (26 %) are major components, whereas Zn-montmorillonite had a predominant fit in the spots analyzed by μ-XANES. Zinc can form a mononuclear inner-sphere complex at the edges of montmorillonite layers at low $[Si]_{aq}$ at approximately 70 μM and precipitates epitaxially as kerolite in relevant geochemical systems with concentrations around 500 μM (Schlegel and Manceau, 2006). Zn-kerolite has been identified in many soils and sediments and is derived from the in-situ weathering of primary minerals (Jacquat et al., 2008; Kirpichtchikova et al., 2006; Manceau et al., 2000; Panfili et al., 2005; van Damme et al., 2010).

The prevalence of the Zn-montmorillonite standard in the fit is consistent with the presence of Zn^{2+} adsorbed on this secondary mineral, which was identified by XRD analysis in our soil sample (Fig. 2). It may be possible to concentrate this type of clay mineral in open-pit mines or during the ore concentration process. Zinc may be incorporated or sorbed on the octahedral sheet or a hydroxy-Al sheet in the interlayer region in the phyllosilicates (Scheinost et al., 2002). Schuwirth et al. (2007) investigated the speciation of Zn in soil layers at a former tailings pond of a Zn/Pb/Ag

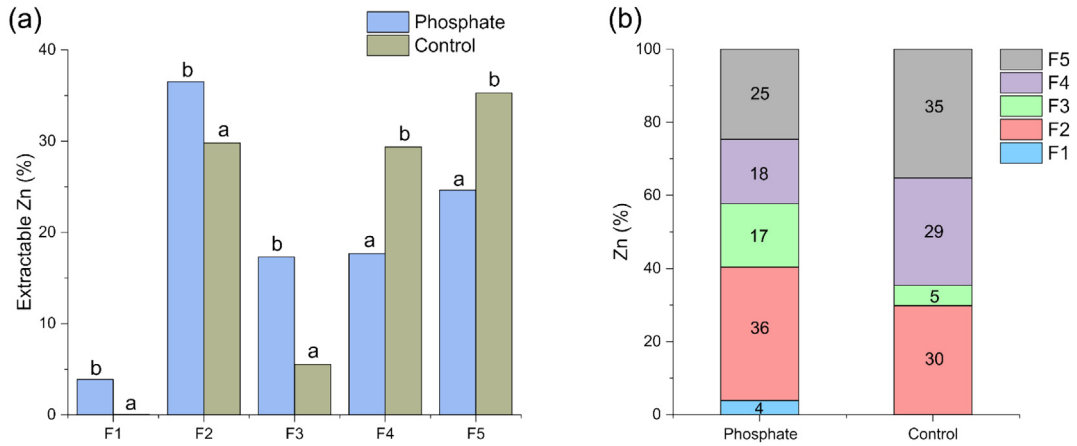

Fig. 5. (a) Relative distributions of Zn among the soil fractions. F1: extractable, F2: bound to carbonates, F3: bound to organic matter, F4: bound to (oxyhydr)oxides, and F5: residual. The column followed the same letter in the same fraction did not differ (*t*-test, $p < 0.05$). (b) Details of Zn pool changes after phosphate addition.

ore mine in the northern Rhineland-Palatinate, Germany, and observed that Zn species was predominantly in the form of Zn adsorbed on montmorillonite and Zn-rich phyllosilicates in the most superficial layer (4 to 6 cm).

Zn-ferrihydrite (24 % of total Zn) and gahnite (10 %) were identified as minor components in the bulk Zn K-edge XANES spectrum. Zn-ferrihydrite is usually detected with phyllosilicates and frequently occurs as a background species in soil matrices (Hochella et al., 1999; Manceau et al., 2002). Similarly, gahnite which is a primary mineral formed mainly in metamorphic high temperature (Hochella et al., 1999) environments was identified in soils impacted by the dust of smelting activities (Isaure et al., 2002; Panfili et al., 2005), and acid mine drainage sites (Hochella et al., 1999). The partial correlations with Fe, and Si are further evidence of the presence of Zn associated with phyllosilicates and ferrihydrite that were identified in the unamended soil.

Similar results were found by Minkina et al. (2018), that verified phases associated with Fe/Mn phyllosilicates and (oxyhydr)oxides as the main stabilizers of Zn mobility. In addition, Minkina et al. (2018) used extended X-ray absorption fine structure (EXAFS) to observe that 70 % of the Zn was linked by single bonds to S, 30 % of the Zn was linked by single bonds to O and that these bonds occurred under alkaline conditions with a high content of sulfate ions. Although we did not find bonds to S, it does not exclude the possibility that part of the sulfate or even other anions formed ionic pairs or precipitates with Zn.

The P-amended soil was the only one that affected the bulk XANES spectrum (Fig. 1). This treatment had a fit with 15 % ZnO, 49 % $Zn_3(PO_4)_2$, and 16 % Zn-LDH. Baker et al. (2012) evaluated the effect of sources of P, reaction times, and distance of the application in the Zn speciation in contaminated soil from an abandoned Pb/Zn smelter near Dearing, KS, USA. Baker et al. (2012) verified the formation of Zn phosphate species and ZnO (zincite) due to P application in certain treatments. Although our LCF result for the control did not show the fit with Zn-LDH, it could still be present in the sample because it is common for Zn-LDH to be identified in soils with pH near 7 and high concentration of Zn (Jacquat et al., 2008; Manceau et al., 2000; Voegelin et al., 2011).

The fit with ZnO is not reasonable because this species is more soluble than Zn-kerolite and Zn-montmorillonite (Voegelin et al., 2011). However, it could probably form as a result of the decrease in pH caused by the amendment (Table 1). As pH decreases, Zn solubility increases (Lindsay, 1979). We did not observe a fit with Zn-kerolite, Zn-montmorillonite, nor Zn-ferrihydrite in the samples amended with phosphate. The non-fit with these minerals is either due to the instability of the Zn-kerolite under acidic conditions (Manceau et al., 2000), the way in which Zn sorption occurs in montmorillonite (electrostatic) (Lothenbach et al., 1997), or Zn sorption in highly pH-dependent ferrihydrite (Dzombak and Morel, 1990).

Micro-XRF and μ-XANES confirmed the formation of $Zn_3(PO_4)_2$ in the P-amended soil (Fig. 3; Table 2). In the μ-XRF image, P is co-localized with Zn, and the significant partial correlation confirmed this association. Micro-XANES showed that the Zn-P species was dominant in most of the spots analyzed. In certain spots, we identified scholzite (Zn,Ca-phosphate), which is a more stable species than Hopeite but requires Ca to be present for such formation (Nriagu, 1984). We also identified Zn-montmorillonite (7 %) and Zn-ferrihydrite (4 %) in some μ-XANES spots, which indicate that these species are present in the amended soil but are not sufficiently abundant to be detected by the bulk XANES. The average of the ten μ-XANES had 32 % $Zn_3(PO_4)_2$, 10 % scholzite, 12 % ZnO, 19 % gahnite, and 27 % Zn-LDH, the species that had fit had the same identified in the bulk XANES except for scholzite.

Nickel, Mn, Pb, and Fe had the highest partial correlation in the P-amended soil (Table A.2). Iron and Mn oxides have a high affinity for Zn and represent two reactive surfaces with which Zn may interact in the soil environment (Voegelin et al., 2002). Karna et al. (2016) found high positive correlation between Zn and Pb, Fe, and Mn in mine waste materials. According to Karna et al. (2016), Zn and Pb could be adsorbed and co-precipitated with Mn and Fe hydr(oxides). Kirpichtchikova et al. (2006) also reported positive correlation between Zn and Pb with Fe in ferruginous clay particles. However, Kirpichtchikova et al. (2006) found no correlation between Zn and Pb with Fe in spots that had low Fe concentration, suggesting that different regions engendered different Zn and Pb species.

The Ni "hot spot" (spot 4 on Zn μ-XRF map; Fig. 3a) was co-localized with the Zn "hot spot". The μ-XANES showed the predominance of Zn-LDH (100 %) at this spot where Ni and Zn could be precipitated on the mineral surface. Nickel can form an Ni-Al layered double hydroxide (Ni-Al-LDH) which precipitates upon the reaction of Ni with montmorillonite, kaolinite, pyrophyllite and gibbsite.

Desorption kinetics and the sequential extraction confirmed the increased Zn plant availability in the P-amended soil samples (Fig. 4). More Zn was desorbed during the initial time of the desorption, which could be inferred from increased Zn extracted in the first fractions (F1, F2, and F3) of the sequential extraction. The first Zn species were probably released from ZnO, and Zn-phosphate followed by Zn-ferrihydrite and Zn-phyllosilicates which were identified by μ-XANES and bulk XANES. Kirpichtchikova et al. (2006) performed an EXAFS with linear combination data either before or after the chemical extraction with EDTA and observed that Zn-phosphate was entirely and selectively dissolved by EDTA. According to Kirpichtchikova et al. (2006), the lower extraction level measured for Zn is due to the Zn-phyllosilicate component, which is less soluble than Zn-phosphate and Zn-ferrihydrite.

Baker et al. (2012) investigated the potential remediation of Pb and Zn after the application of fluid phosphoric acid (PA), ammonium polyphosphate, granular rock phosphate, triple superphosphate, and monoammonium phosphate. Baker et al. (2012) found that the addition of PA was not efficient in forming the zinc phosphate species due to the increased solubility of Zn generated by the application of phosphoric acid. The formation of stable metallic phosphates in the soil is affected by soil pH, mineral composition, presence of soil organic matter, soil biota, and other environmental parameters (Debela et al., 2013). Zahedifar (2017) observed that the application of 1.5 % of biochar increased soil pH and Zn associated with carbonate (F2), but reduced the contents of exchangeable Zn (F1). For this amendment, however, the rate was a crucial factor in Zn immobilization because the application of a higher rate (3 %) reduced the F2 fraction of Zn.

Wu et al. (2013) verified that the application of 2283 mg kg^{-1} of K_2HPO_4, $Ca_3(PO_4)_2$, $Ca_5(PO_4)_3OH$, and $Ca(H_2PO_4)_2{\cdot}2H_2O$ was effective in reducing the exchangeable content of Zn (F1). Wu et al. (2013) concluded that the phosphate source affected the residual fraction (F5) (K_2HPO_4 reduced the Zn content) and that the source altered soil pH and, consequently, the Zn fraction associated with carbonate. The addition of K_2HPO_4 increased the soil pH by two units (final pH 7.9) and was the treatment that most reduced the exchangeable Zn content (F1). The effectiveness of the remediation observed by the TCLP test indicated the greatest stability in the immobilization of Zn through the addition of $Ca_5(PO_4)_3OH$.

The success in metal retention by phosphate remediation is also related to the binding mechanisms and the sorption preference of phosphate in metals. Cao et al. (2004) observed that the application of phosphate rock had a greater affinity for sorbing first Pb (78 %), then Cu (25 %), and finally Zn (4 %). In that same study, Cao et al. (2004) found that, in addition to the preference for sorption sites, pH sensitivity can be a key factor for the immobilization of Cu and Zn.

Dissolved metals are found in the soil solution as organic complexes, inorganic complexes, and/or free (un-complexed) metals. The free metal compartment, in general, is relatively smaller compared to other forms in solution or pools of metal in the solid phase. The proportion of free Zn pool can increase considerably in solution as soil pH decreases. Free metal is considered the most reactive form of metal in soil and is fundamental to remediation strategies for understanding and predicting its mobility, toxicity, and bioavailability in soil and water (Mhalla et al., 2021).

4.2. Environmental recommendations

The city of Vazante has one of the major non-sulfide zinc deposits in the world (Hitzman et al., 2003; Soares Monteiro et al., 2006), with

hemimorphite ($Zn_4Si_2O_7(OH)_2{\cdot}H_2O$) and willemite ($Zn_2SiO_4$) having been previously reported in this region (Virgínia et al., 2007). In our experiment, the P application (46.4 g of $NH_4H_2PO_4$ per kg of soil) increased Zn availability due to the formation of species such as ZnO that could be easily released.

Many researchers focused on using P sources to remediate heavy metal contamination with phosphate, such as the application of KH_2PO_4 or H_3PO_4 (Andrunik et al., 2020; Austruy et al., 2014; Cao et al., 2013). As the effectiveness of crude phosphate rocks is generally low, researchers have used other phosphate sources or have modified the phosphate rocks so as to release more soluble P. In our study, we evaluated the main species of Zn formed after remediation with phosphate and observed that $NH_4H_2PO_4$ played a fundamental role in reducing the pH, which led to the release of Zn from stable phases at pHs in the alkaline range.

In the pH close to 6.5, the sequential extraction showed that part of the Zn was associated with carbonated fractions, which was not possible to prove with the XAS analysis. Therefore, this may indicate that secondary phases, thermodynamically stable at circumneutral pH, may be acting in the release of Zn to the environment. So, pH may be a key factor in Zn mobility in the long term. This information is exceptionally important in helping to develop remediation strategies that provide a cost-effective and sustainable solution. For future studies, we recommend that the long-term change in pH and availability of Zn after remediation with phosphate be evaluated, especially when the P source contains ammonium.

5. Conclusions

The application of mono-ammonium phosphate decreased the recalcitrant forms of Zn and increased the exchangeable and available fractions, which were accessed by sequential fractionation. This application, however, was not suitable for remediation of Zn in the soil as it increased the mobilization of the element in the soil.

The XAS analysis evidenced the reduction in the gahnite and montmorillonite species, suggesting the dissolution of these species was a function of pH reduction.

The increase in Zn mobility was confirmed by desorption kinetics, indicating an increase in soluble Zn after the application of mono-ammonium phosphate.

CRediT authorship contribution statement

Gomes FP: Conceptualization, Methodology, Formal analysis and Data processing, Investigation, Writing - Original Draft, Review & Editing; **Soares MB**: Formal analysis and Data processing, Investigation, Writing - Original Draft, Review & Editing; **Carvalho HWP**: Methodology, Formal analysis and Data processing, Investigation, Writing - Original Draft, Review & Editing; **Sharma A**: Formal analysis and Data processing, Investigation, Writing - Original Draft, Review & Editing; **Hesterberg D**: Methodology, Formal analysis and Data processing, Investigation, Writing - Original Draft, Review & Editing; **Alleoni LRF**: Supervision, Funding acquisition and Writing - Review & Editing.

Data availability

Data will be made available on request.

Declaration of competing interest

The authors declare that they have no known competing financial interests or personal relationships that could have appeared to influence the work reported in this paper.

Acknowledgments

The 1st author gratefully thanks the São Paulo Research Foundation (FAPESP) (grants #2016/13734-0 and #2017/11700-4) for the scholarships granted for this research. The 2nd author gratefully thanks the FAPESP (grant #2019/06897-9) for the scholarships granted for this research. The 6th author thanks CNPq (grant #306429/2018-7) for the scholarship granted for this research. This research used facilities of the Brazilian Synchrotron Light Laboratory (LNLS), part of the Brazilian Center for Research in Energy and Materials (CNPEM), a private non-profit organization under the supervision of the Brazilian Ministry for Science, Technology, and Innovations (MCTI). The D09B-XRF and XAFS2 beamlines staff is acknowledged for the assistance during the experiments [20180460 and 20170360]. Also, this research used resources [5-ID Beamline] of the National Synchrotron Light Source II, a U.S. Department of Energy (DOE) Office of Science User Facility operated for the DOE Office of Science by Brookhaven National Laboratory under Contract No. DE-SC0012704. The authors also thank the researchers Aesar, A., Hettiarachchi, G. M., McLaughlin, M. J., Scheckel, K. G., Chittleborough, D. J., Newville, M., Sutton, S., Lombi, E, Nachtegaal, M., Marcus, M. A., Sonke, J. E., Vangronsveld, J., Livi, K. J. T., van Der Lelie, D., Sparks, D. L., Baker, L. R., and Pierzynski, G. M. for providing the zinc standards used in the XANES analysis. The authors are also thankful to Professor Leônidas Carrijo Melo and Professor Luiz Roberto Guimarães Guilherme, from the Soil Science Department at the Federal University of Lavras (Brazil), for kindly having made available the soil samples used in this study, and Professor Leonardus Vergütz, from the Mohammed VI Polytechnic University (Morocco), for the support in the stirred-flow analysis.

Appendix A. Supplementary data

Supplementary data to this article can be found online at https://doi.org/10.1016/j.scitotenv.2022.161009.

References

Abdelhafez, A.A., Li, J., Abbas, M.H.H.H., 2014. Feasibility of biochar manufactured from organic wastes on the stabilization of heavy metals in a metal smelter contaminated soil. Chemosphere 117, 66–71. https://doi.org/10.1016/j.chemosphere.2014.05.086.

Andrunik, M., Wołowiec, M., Wojnarski, D., Zelek-Pogudz, S., Bajda, T., 2020. Transformation of Pb, Cd, and Zn minerals using phosphates. Minerals 10, 342. https://doi.org/10.3390/MIN10040342.

Appel, C., 2002. Concentration, pH, and surface charge effects on cadmium and Lead sorption in three tropical soils. J. Environ. Qual. 31, 581–589.

Austruy, A., Shahid, M., Xiong, T., Castrec, M., Payre, V., Niazi, N.K., Sabir, M., Dumat, C., 2014. Mechanisms of metal-phosphates formation in the rhizosphere soils of pea and tomato: environmental and sanitary consequences. J. Soils Sediments 14, 666–678. https://doi.org/10.1007/S11368-014-0862-Z/FIGURES/5.

Baker, L.R., Pierzynski, G.M., Hettiarachchi, G.M., Scheckel, K.G., Newville, M., 2014. Micro-X-ray fluorescence, micro-X-ray absorption spectroscopy, and micro-X-ray diffraction investigation of Lead speciation after the addition of different phosphorus amendments to a smelter-contaminated soil. J. Environ. Qual. 43, 488. https://doi.org/10.2134/jeq2013.07.0281.

Baker, L.R., Pierzynski, G.M., Hettiarachchi, G.M., Scheckel, K.G., Newville, M., 2012. Zinc speciation in proximity to phosphate application points in a Lead/Zinc smelter-contaminated soil. J. Environ. Qual. 41, 1865–1873. https://doi.org/10.2134/jeq2012.0168.

Basta, N.T., McGowen, S.L., 2004. Evaluation of chemical immobilization treatments for reducing heavy metal transport in a smelter-contaminated soil. Environ. Pollut. 127, 73–82. https://doi.org/10.1016/S0269-7491(03)00250-1.

Brasil, 2011. National Solid Waste Plan. Lei no 12.305/2010). Diário Oficial da União 103, Brasilia in Portuguese.

Cao, X., Liang, Y., Zhao, L., Le, H., 2013. Mobility of pb, cu, and zn in the phosphorus-amended contaminated soils under simulated landfill and rainfall conditions. Environ. Sci. Pollut. Res. 20, 5913–5921. https://doi.org/10.1007/S11356-012-1349-3/FIGURES/6.

Cao, X., Ma, L.Q., Rhue, D.R., Appel, C.S., 2004. Mechanisms of lead, copper, and zinc retention by phosphate rock. Environ. Pollut. 131, 435–444. https://doi.org/10.1016/J.ENVPOL.2004.03.003.

Debela, F., Arocena, J.M., Thring, R.W., Whitcombe, T., 2013. Organic acids inhibit the formation of pyromorphite and Zn-phosphate in phosphorous amended Pb- and Zn-contaminated soil. J. Environ. Manag. 116, 156–162. https://doi.org/10.1016/J.JENVMAN.2012.11.037.

Dzombak, D.A., Morel, F., 1990. Surface Complexation Modeling: Hydrous Ferric Oxide. Wiley.

Fang, Y., Cao, X., Zhao, L., 2012. Effects of phosphorus amendments and plant growth on the mobility of Pb, Cu, and Zn in a multi-metal-contaminated soil. Environ. Sci. Pollut. Res. 19, 1659–1667. https://doi.org/10.1007/s11356-011-0674-2.

Fellet, G., Marchiol, L., Delle Vedove, G., Peressotti, A., 2011. Application of biochar on mine tailings: effects and perspectives for land reclamation. Chemosphere 83, 1262–1267.

Filho, A.A.Q., Neto, A.A.A., Dantas, J.O.C., 2015. Mineral Summary 2015: Gipsita. 35, pp. 72–73 in Portuguese.
Goh, K.-H., Lim, T.-T., 2004. Geochemistry of inorganic arsenic and selenium in a tropical soil: effect of reaction time, pH, and competitive anions on arsenic and selenium adsorption. Chemosphere 55, 849–859. https://doi.org/10.1016/J.CHEMOSPHERE.2003.11.041.
Hitzman, M.W., Reynolds, N.A., Sangster, D.F., Allen, C.R., Carman, C.E., 2003. Classification, genesis, and exploration guides for nonsulfide zinc deposits. Econ. Geol. 98, 685–714. https://doi.org/10.2113/gsecongeo.98.4.685.
Hochella, M.F., Moore, J.N., Golla, U., Putnis, A., 1999. A TEM study of samples from acid mine drainage systems: metal-mineral association with implications for transport. Geochim. Cosmochim. Acta 63, 3395–3406. https://doi.org/10.1016/S0016-7037(99)00260-4.
Hosseiwwnpur, A.R., Motaghian, H., 2015. Evaluating of many chemical extractants for assessment of Zn and Pb uptake by bean in polluted soils. 15, 24–34.
Ingram, J.S.I., Anderson, J.M.(Jonathan M.)., 1993. Tropical Soil Biology and Fertility: A Handbook of Methods. CAB International.
Isaure, M.P., Laboudigue, A., Manceau, A., Sarret, G., Tiffreau, C., Trocellier, P., Lamble, G., Hazemann, J.L., Chateigner, D., 2002. Quantitative zn speciation in a contaminated dredged sediment by μ-PIXE, μ-SXRF, EXAFS spectroscopy and principal component analysis. Geochim. Cosmochim. Acta 66, 1549–1567. https://doi.org/10.1016/S0016-7037(01)00875-4.
Jacquat, O., Voegelin, A., Villard, A., Marcus, M.A., Kretzschmar, R., 2008. Formation of zn-rich phyllosilicate, zn-layered double hydroxide and hydrozincite in contaminated calcareous soils. Geochim. Cosmochim. Acta 72, 5037–5054. https://doi.org/10.1016/j.gca.2008.07.024.
Kampf, N., Schwertmann, U., 1982. The 5-M-NaOH concentration treatment for iron oxides in soils. Clay Clay Miner. 30, 401–408.
Karna, R.R., Hettiarachchi, G.M., Newville, M., Sun, C., Ma, Q., 2016. Synchrotron-based X-ray spectroscopy studies for redox-based remediation of Lead, zinc, and cadmium in mine waste materials. J. Environ. Qual. 45, 1883. https://doi.org/10.2134/jeq2015.12.0616.
Kirpichtchikova, T.A., Manceau, A., Spadini, L., Panfili, F., Marcus, M.A., Jacquet, T., 2006. Speciation and solubility of heavy metals in contaminated soil using X-ray microfluorescence, EXAFS spectroscopy, chemical extraction, and thermodynamic modeling. Geochim. Cosmochim. Acta 70, 2163–2190. https://doi.org/10.1016/j.gca.2006.02.006.
Lee, S.H., Lee, J.S., Jeong Choi, Y., Kim, J.G., 2009. In situ stabilization of cadmium-, lead-, and zinc-contaminated soil using various amendments. Chemosphere 77, 1069–1075. https://doi.org/10.1016/j.chemosphere.2009.08.056.
Lindsay, W.L., 1979. Chemical equilibria in soils. Chemical Equilibria in Soils.
Lothenbach, B., Furrer, G., Schulin, R., 1997. Immobilization of Heavy Metals by Polynuclear Aluminium and Montmorillonite Compounds. https://doi.org/10.1021/ES960697H.
Manceau, A., Lanson, B., Schlegel, M.L., Hargé, J.C., Musso, M., Eybert-Bérard, L., Hazemann, J.L., Chateigner, D., Lamble, G.M., 2000. Quantitative ZN speciation in smelter-contaminated soils by EXAFS spectroscopy. Am. J. Sci. 300, 289–343. https://doi.org/10.2475/ajs.300.4.289.
Manceau, A., Marcus, M.A., Grangeon, S., 2012. Determination of Mn valence states in mixed-valent manganates by XANES spectroscopy. Am. Mineral. 97, 816–827. https://doi.org/10.2138/am.2012.3903.
Manceau, A., Marcus, M.A., Tamura, N., 2002. Quantitative speciation of heavy metals in soils and sediments by synchrotron X-ray techniques. Rev. Mineral. Geochem. 49, 341–428. https://doi.org/10.2138/gsrmg.49.1.341.
McBride, M.B., 1994. Environmental Chemistry of Soils. Oxford University Press.
McBride, M.B., Blasiak, J.J., 1979. Zinc and copper solubility as a function of pH in an acid soil. Soil Sci. Soc. Am. J. 43, 866–870. https://doi.org/10.2136/SSSAJ1979.03615995004300050009X.
Mehra, O.P., Jackson, M.L., 1960. Iron oxide removal from soils and clays by a dithionite-citrate system buffered with sodium bicarbonate. Clay Clay Miner. 317–327. https://doi.org/10.1016/B978-0-08-009235-5.50026-7.
Mhalla, B., Ahmed, N., Datta, S.P., Golui, D., Singh, M., Shrivastava, M., 2021. Solubility Relationship of Metals in Acid Soils of Kumaon Himalaya Region of India. 52, pp. 2373–2387. https://doi.org/10.1080/00103624.2021.1928170.
Minca, K.K., Basta, N.T., Scheckel, K.G., 2014. Using the Mehlich-3 Soil Test as an Inexpensive Screening Tool to Estimate Total and Bioaccessible Lead in Urban Soils. 1526, pp. 1518–1526. https://doi.org/10.2134/jeq2012.0450 in Portuguese.
Minkina, T., Nevidomskaya, D., Bauer, T., Shuvaeva, V., Soldatov, A., Mandzhieva, S., Zubavichus, Y., Trigub, A., 2018. Determining the speciation of zn in soils around the sediment ponds of chemical plants by XRD and XAFS spectroscopy and sequential extraction. Sci. Total Environ. 634, 1165–1173. https://doi.org/10.1016/J.SCITOTENV.2018.04.118.
Nawab, J., Khan, S., Aamir, M., Shamshad, I., Qamar, Z., Din, I., Huang, Q., 2016. Organic amendments impact the availability of heavy metal(loid)s in mine-impacted soil and their phytoremediation by penisitum americanum and Sorghum bicolor. Environ. Sci. Pollut. Res. 23, 2381–2390. https://doi.org/10.1007/s11356-015-5458-7.
Nriagu, J.O., 1984. Formation and stability of base metal phosphates in soils and sediments. Phosphate Minerals. Springer Berlin Heidelberg, Berlin, Heidelberg, pp. 318–329 https://doi.org/10.1007/978-3-642-61736-2_10.
Panfili, F., Manceau, A., Sarret, G., Spadini, L., Kirpichtchikova, T., Bert, V., Laboudigue, A., Marcus, M.A., Ahamdach, N., Libert, M.-F., 2005. The effect of phytostabilization on zn speciation in a dredged contaminated sediment using scanning electron microscopy, X-ray fluorescence, EXAFS spectroscopy, and principal components analysis. Geochim. Cosmochim. Acta 69, 2265–2284. https://doi.org/10.1016/J.GCA.2004.10.017.
Puga, A.P., Abreu, C.A., Melo, L.C.A., Beesley, L., 2015. Biochar application to a contaminated soil reduces the availability and plant uptake of zinc, lead and cadmium. J. Environ. Manag. 159, 86–93. https://doi.org/10.1016/J.JENVMAN.2015.05.036.
Roberts, D.R., Scheinost, A.C., Sparks, D.L., 2002. Zinc Speciation in a Smelter-contaminated Soil Profile Using Bulk and Microspectroscopic Techniques. https://doi.org/10.1021/ES015516C.
Scheinost, A.C., Kretzschmar, R., Pfister, S., Darryl, R.R., 2002. Combining Selective Sequential Extractions, X-ray Absorption Spectroscopy, and Principal Component Analysis for Quantitative Zinc Speciation in Soil. https://doi.org/10.1021/ES025669F.
Schlegel, M.L., Manceau, A., 2006. Evidence for the nucleation and epitaxial growth of Zn phyllosilicate on montmorillonite. Geochim. Cosmochim. Acta 70, 901–917. https://doi.org/10.1016/j.gca.2005.10.021.
Schuwirth, N., Voegelin, A., Kretzschmar, R., Hofmann, T., 2007. Vertical distribution and speciation of trace metals in weathering flotation residues of a zinc/lead sulfide mine. J. Environ. Qual. 36, 61–69. https://doi.org/10.2134/jeq2006.0148.
Seshadri, B., Bolan, N.S., Choppala, G., Kunhikrishnan, A., Sanderson, P., Wang, H., Currie, L.D., Tsang, D.C.W., Ok, Y.S., Kim, G., 2017. Potential value of phosphate compounds in enhancing immobilization and reducing bioavailability of mixed heavy metal contaminants in shooting range soil. Chemosphere 184, 197–206. https://doi.org/10.1016/J.CHEMOSPHERE.2017.05.172.
Sharma, A., Muyskens, A., Guinness, J., Polizzotto, M.L., Fuentes, M., Tappero, R.V., Chen-Wiegart, Y.C.K., Thieme, J., Williams, G.J., Acerbo, A.S., Hesterberg, D., 2019. Multi-element effects on arsenate accumulation in a geochemical matrix determined using μ-XRF, μ-XANES and spatial statistics. J. Synchrotron. Radiat. 26, 1967–1979. https://doi.org/10.1107/S1600577519012785.
Sharma, S., Kaur, I., Nagpal, A.K., 2018. Estimation of arsenic, manganese and iron in mustard seeds, maize grains, groundwater and associated human health risks in ropar wetland, Punjab, India, and its adjoining areas. Environ. Monit. Assess. 190, 385. https://doi.org/10.1007/s10661-018-6763-7.
Sidhu, V., Sarkar, D., Datta, R., 2016. Effects of biosolids and compost amendment on chemistry of soils contaminated with copper from mining activities. Environ. Monit. Assess. 188, 176. https://doi.org/10.1007/s10661-016-5185-7.
Sik Ok, Y., Lim, J.E., Moon, D.H., 2011. Stabilization of Pb and Cd contaminated soils and soil quality improvements using waste oyster shells. Environ. Geochem. Health 33, 83–91. https://doi.org/10.1007/s10653-010-9329-3.
Silveira, M.L., Alleoni, L.R.F., O'Connor, G.A., Chang, A.C., 2006. Heavy metal sequential extraction methods-a modification for tropical soils. Chemosphere 64, 1929–1938. https://doi.org/10.1016/j.chemosphere.2006.01.018.
Sims, J.T., 1986. Soil pH effects on the distribution and plant availability of manganese, copper, and zinc. In: Horwath, W. (Ed.), Soil Science Society of America Journal. John Wiley & Sons Ltd, pp. 367–373 https://doi.org/10.2136/SSSAJ1986.03615995005000020023X.
Soares Monteiro, L.V., Bettencourt, J.S., Juliani, C., de Oliveira, T.F., 2006. Geology, petrography, and mineral chemistry of the Vazante non-sulfide and Ambrósia and Fagundes sulfide-rich carbonate-hosted Zn–(Pb) deposits, Minas Gerais, Brazil. Ore Geol. Rev. 28, 201–234. https://doi.org/10.1016/J.OREGEOREV.2005.03.005.
Soil Survey Staff, 2014. Keys to Soil Taxonomy. 12th ed. NRCS, Washington.
Steinnes, E., 1995. Heavy metals in soils. Heavy Metals in Soils. Springer, Netherlands, Dordrecht https://doi.org/10.1007/978-94-011-1344-1.
USEPA, 2007. Method 3051A: Microwave Assisted Acid Digestion of Sediments, Sludges, Soils and Oils. EPA, Washington.
van Damme, A., Degryse, F., Smolders, E., Sarret, G., Dewit, J., Swennen, R., Manceau, A., 2010. Zinc speciation in mining and smelter contaminated overbank sediments by EXAFS spectroscopy. Geochim. Cosmochim. Acta 74, 3707–3720. https://doi.org/10.1016/J.GCA.2010.03.032.
Virgínia, L., Monteiro, S., Silva, J., Juliani, C., Flávio, T., Oliveira, D., 2007. Nonsulfide and sulfide-rich zinc mineralizations in the Vazante, Ambrósia and Fagundes deposits, Minas Gerais, Brazil: mass balance and stable isotope characteristics of the hydrothermal alterations. 11, 362–381. https://doi.org/10.1016/j.gr.2006.04.017.
Voegelin, A., Jacquat, O., Pfister, S., Barmettler, K., Scheinost, A.C., Kretzschmar, R., 2011. Time-dependent changes of zinc speciation in four soils contaminated with zincite or sphalerite. Environ. Sci. Technol. 45, 255–261. https://doi.org/10.1021/es101189d.
Voegelin, A., Scheinost, A.C., Bühlmann, K., Barmettler, K., Kretzschmar, R., 2002. Slow formation and dissolution of zn precipitates in soil: a combined column-transport and XAFS study. Environ. Sci. Technol. 36, 3749–3754. https://doi.org/10.1021/es010316m.
WRB, 2014. World Reference Base for Soil Resources. FAO, Rome.
Wu, W.H., Xie, Z.M., Xu, J.M., Wang, F., Shi, J.C., Zhou, R.Bin, Jin, Z.F., 2013. Immobilization of trace metals by phosphates in contaminated soil near lead/zinc mine tailings evaluated by sequential extraction and TCLP. J. Soils Sediments 13, 1386–1395. https://doi.org/10.1007/S11368-013-0751-X/TABLES/3.
Yin, Y., Allen, H.E., Huang, C.P., Sparks, D.L., Sanders, P.F., 1997. Kinetics of mercury(II) adsorption and desorption on soil. Environ. Sci. Technol. 31, 496–503. https://doi.org/10.1021/es9603214.
Zahedifar, M., 2017. Sequential extraction of zinc in the soils of different land use types as influenced by wheat straw derived biochar. J. Geochem. Explor. 182, 22–31. https://doi.org/10.1016/J.GEXPLO.2017.08.007.